Journal of Organometallic Chemistry 723 (2013) 79–89

Contents lists available at SciVerse ScienceDirect

Journal of Organometallic Chemistry

journal homepage: www.elsevier.com/locate/jorganchem

Synthesis, spectroscopic characterization, X-ray structures, biological screenings, DNA interaction study and catalytic activity of organotin(IV) 3-(4-flourophenyl)-2-methylacrylic acid derivatives

Muhammad Tariq [a], Niaz Muhammad [b], Muhammad Sirajuddin [a], Saqib Ali [a,*], Naseer Ali Shah [d], Nasir Khalid [c], Muhammad Nawaz Tahir [e], Muhammad Rashid Khan [d]

[a] Department of Chemistry, Quaid-i-Azam University, 45320 Islamabad, Pakistan
[b] Department of Chemistry, Abdul Wali Khan University, Mardan, Pakistan
[c] Chemistry Division, Pakistan Institute of Nuclear Science and Technology, P.O. Nilore, Pakistan
[d] Department of Biochemistry, Quaid-i-Azam University, Islamabad 45320, Pakistan
[e] Department of Physics, University of Sargodha, Pakistan

ARTICLE INFO

Article history:
Received 30 July 2012
Received in revised form
13 September 2012
Accepted 18 September 2012

Keywords:
Organotin(IV) carboxylate
Antimicrobial activity
Antitumor activity
Cytotoxicity
DNA interaction
Catalytic activity

ABSTRACT

A series of organotin(IV) carboxylate complexes $[Me_2SnL_2]$ (**1**), $[Bu_2SnL_2]$ (**2**), $[Oct_2SnL_2]$ (**3**), $[Me_3SnL]$ (**4**), $[Bu_3SnL]$ (**5**) and $[Ph_3SnL]$ (**6**), where $L = O_2C(CH_3)C{=}CHC_6H_4F$ have been successfully synthesized and characterized by FT-IR, NMR (^1H, ^{13}C) and single crystal analysis. The ligand coordinates to tin atom via carboxylate group. Compound **1** and **4** have also been studied by single crystal XRD analysis. The synthesized compounds were screened for their biological activities including anti-bacterial, anti-fungal, anti-tumor and cytotoxicity. The compounds **4**–**6** exhibit excellent anti-bacterial, anti-fungal and anti-tumor activities. The ligand binds with DNA double helix by hydrogen bonding between the ligand and the base pairs in DNA typically to N3 of adenine and O2 of thymine as well as partial intercalation of aromatic ring into the base pairs of DNA. The complexes also interact with DNA via intercalation of aromatic ring into the base pairs of DNA. The catalytic activity of compounds **46** was assessed in transesterification of triglycerides in rocket seed oil into biodiesel. The choice of these compounds is the Lewis acid nature of tin atom. The samples were taken in regular interval of 1, 8, 16 and 24 h and % age conversion was determined by ^1H NMR. All the tested compounds showed good catalytic activity in the order **4** > **5** > **6**.

1. Introduction

The organotin(IV) carboxylates have been shown significant antimicrobial properties such as anti-bacterial and anti-fungal [1,2]. The organotin compounds have also received considerable attention as anti-tumor and anti-cancer drugs. The activity is due to dissociated organotin(IV) moieties [3]. The biological activity usually associates with the nature of organic ligand [4,5], since the organic ligand facilitates the transportation of the complexes across the cell membrane. Spectroscopic characterizations have confirmed a great structural variety for organotin(IV) carboxylates both in solid and solution states. The versatile structural ability is related to mode of binding of COO^- moiety. The well known natures of their bonding are mono, di, tetra and oligomeric ladder, cyclic or hexameric structure [6–8]. Organotin carboxylates have also a wide range of industrial applications as catalysts for esterification and transesterification [9,10], silicone curing [11], formation of polyurethane [12], antifouling paints [13–15], PVC stabilization [16], as homogeneous catalysts [17], and as ion carriers in electrochemical membranes design [18,19]. Very few reports are available in literature regarding the use of organotin carboxylates for the transesterification of vegetable oil into biodiesel. Biodiesel is the monoalkyl ester of long chain fatty acids derived from the renewable feed stock, such as vegetable oil or animal fats and is usually produced by a transesterification of vegetable oil with methanol [20–23]. The triglycerides in oil are being transesterified with base catalysts like NaOH, KOH etc [24–26] but these basic catalysts need excessive water washing and neutralization. Heterogeneous catalysts like CaO, MgO, Mg–Al hydrotalcite etc have also been used in transesterification of oils [27–29] but these take more time and

* Corresponding author. Tel.: +92 51 90642130; fax: +92 51 90642241.
E-mail address: drsa54@yahoo.com (S. Ali).

0022-328X/$ – see front matter © 2012 Elsevier B.V. All rights reserved.
http://dx.doi.org/10.1016/j.jorganchem.2012.09.011

higher alcoholic ratio. A very few examples are reported for transesterification of triglycerides with organotin(IV) carboxylates as homogeneous metal catalyst [30–33].

Keeping in view the versatile applications of organotin(IV) carboxylates, in the present study, we have synthesized and characterized 3-(4-flourophenyl)-2-methylacrylic acid and its six organotin(IV) derivatives. These complexes have been screened for their anti-bacterial, anti-fungal, cytotoxicity and anti-tumor activity. DNA interaction studies were also conducted for the synthesized complexes using spectrophotometric technique. The selected organotin(IV) carboxylates have been assessed as catalyst in transesterification of triglycerides to produce biodiesel.

2. Experimental

2.1. Materials and methods

All the diorganotin(IV) and triorganotin(IV) precursors were purchased from Aldrich and were used without further purification. All the solvents used were of analytical grade and dried according to reported procedures before use [34]. The melting points were recorded on a Gallenkamp (UK) electrothermal melting point apparatus. IR spectra were recorded with Thermo Nicolet-6700 FT-IR Spectrophotometer by measuring the absorbance of the samples from 4000 to 400 cm^{-1}. ^1H and ^{13}C NMR spectra were recorded at room temperature in $CDCl_3$ on a Brucker Advance Digital 300 MHz NMR spectrometer (Switzerland). The absorption spectra were recorded on a Shimadzu 1800 UV–vis spectrophotometer. Viscosity for DNA interaction studies of ligand **HL** and representative complexes, was measured by an Ubbelohde viscometer at ambient temperature of 23 ± 1 °C. The X-ray diffraction data were collected on a Bruker SMART APEX CCD diffractometer, equipped with a 4 K CCD detector set 60.0 mm from the crystal. The crystals were cooled to 100 ± 1 K using the Bruker KRYOFLEX low temperature device and intensity measurements were performed using graphite monochromated Mo-Kα radiation from a sealed ceramic diffraction tube (SIEMENS). Generator settings were 50 kV/40 mA. The structure was solved by Patterson method and extension of the model was accomplished by direct method using the program DIRDIF or SIR2004. Final refinement on F2 carried out by full matrix least squares techniques using SHELXL-97, a modified version of the program PLUTO (preparation of illustrations) and PLATON package. The rocket seeds were purchased from a local market. The seeds were washed with distilled water to remove the dirt and were oven dried at 60 °C till constant weight. The oil was extracted by using electric oil expeller (KEK P0015-10127) Germany. Methanol (CH_3OH), sodium hydroxide (NaOH) and anhydrous sodium sulfate (Na_2SO_4) were of analytical grade obtained from Merck (Germany) and used as such. Distilled water was used through out the present studies.

2.2. Synthesis

2.2.1. 3-(4-flourophenyl)-2-methylacrylic acid

A mixture of 4-flourobenzaldehyde (3.47 g, 28.0 mmol), methylmalonic acid (6.60 g, 56.0 mmol) and piperidine (4.76 g, 56.0 mmol) in molar ratios of 1:2:2 was refluxed in pyridine as solvent in two neck round bottom flask on a steam-bath for 24 h (Scheme 1). The reaction mixture was cooled and added to a mixture of concentrated HCl and ice. The precipitate formed in the acidified mixture was filtered off and washed with ice cold water. The product was recrystallized from an alcohol–water mixture (4:1). Yield: 3.68 g, 73.6%. M.p. 152–153 °C. IR (cm^{-1}): 3321–2530 ν(OH), 1675 $\nu(OCO)_{asym}$, 1423 $\nu(OCO)_{sym}$, ($\Delta\nu = 252\ cm^{-1}$). ^1H NMR ($CDCl_3$, ppm): 11.32 (s, H_1, 1H), 7.81 (s, H_3, 1H), 7.10 (d, $H_{5,5'}$, 2H), 7.43 (d, $H_{6,6'}$, 2H), 2.15 (s, H_8, 3H). ^{13}C NMR ($CDCl_3$, ppm): 174.2 (C-1), 127.2 (C-2), 139.9 (C-3), 131.6 (C-4), 127.3 (C-5), 115.4 (C-6), 164.3 (C-7), 13.6 (C-8).

2.2.2. Sodium salt of 3-(4-flourophenyl)-2-methylacrylic acid

The sodium salt of ligand, R/COONa, was prepared by dropwise addition of an equimolar amount of sodium hydrogen carbonate solution to a methanolic solution of acidic ligand (R/COOH). The mixture was stirred for 2 h at room temperature, evaporated under reduced pressure to give a white solid and was vacuum dried.

The following scheme represents numbering in ligand and organic groups attached to Sn atom as shown by ^1H and ^{13}C NMR.

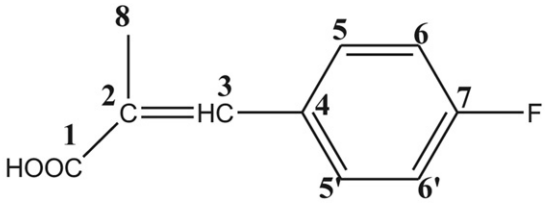

3-(4-fluorophenyl)-2-methylacrylic acid

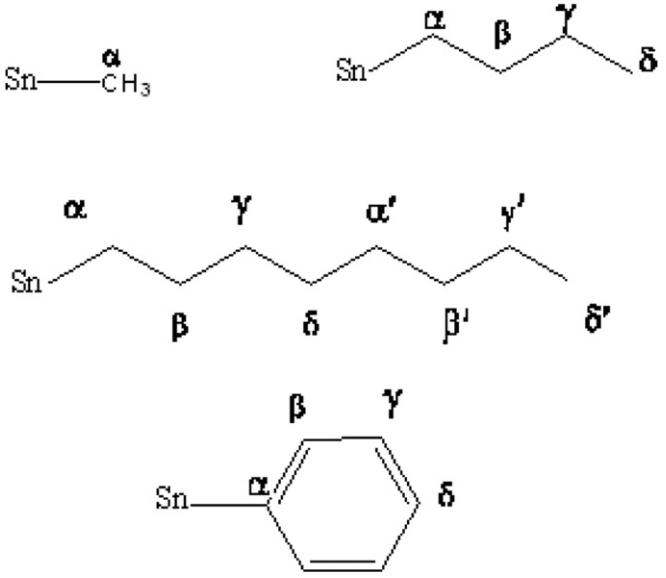

2.2.3. Dimethyltin(IV) [bis(3-(4-flourophenyl)-2-methylacrylate)] (**1**)

The sodium salt R/COONa (0.6 g, 3 mmol), was refluxed for 10 h with dimethyltin(IV) dichloride (0.32 g, 1.5 mmol) in dry toluene in a 250 mL two necked round bottom flask. A turbid solution obtained, was left overnight at room temperature. The sodium chloride formed was filtered off and the filtrate was rotary evaporated. The resultant solid mass was recrystallized from chloroform and *n*-hexane (4:1) mixture. Yield: (0.54 g, 72%). M.p. 159–160 °C. IR (cm^{-1}): 1505 $\nu(OCO)_{asym}$, 1370 $\nu(OCO)_{sym}$, ($\Delta\nu = 135\ cm^{-1}$), 523 ν(Sn–C), 466 ν(Sn–O). ^1H NMR ($CDCl_3$ ppm),: 7.83 (s, H_3, 2H), 7.08 (d, $H_{5,5'}$, 4H), 7.42 (d, $H_{6,6'}$, 4H), 2.17 (s, H_8, 6H), 1.10 (s, Hα, 6H, $^2J(^{119/117}Sn-^1H) = 83/80$ Hz). ^{13}C NMR ($CDCl_3$, ppm): 173.8 (C-1), 131.9 (C-2), 139.0 (C-3), 127.0 (C-4), 131.6 (C-5), 115.4 (C-6), 160.9 (C-7), 14.3 (C-8), 1.0 (C-α).

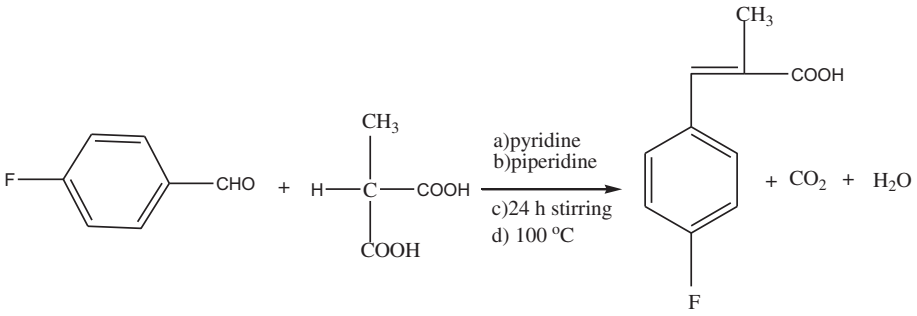

Scheme 1.

*2.2.4. Dibutyltin(IV) [bis(3-(4-flourophenyl)-2-methylacrylate)] (**2**)*

Compound **2** was prepared in the same way as **1**, using R/COONa (0.4 g, 2 mmol) and dibutyltin(IV) dichloride (0.30 g, 1.0 mmol) in 2:1 molar ratios. The product was recrystallized from chloroform and *n*-hexane (4:1) mixture. Yield: (0.45 g, 78%). M.p. 74–75 °C. IR (cm^{-1}): 1507 $\nu(OCO)_{asym}$, 1366 $\nu(OCO)_{sym}$, ($\Delta\nu$ = 141 cm^{-1}), 524 ν(Sn–C), 463 ν(Sn–O). ^{1}H NMR ($CDCl_3$ ppm),: 7.50 (s, H_3, 2H), 7.10 (d, $H_{5,5'}$, 4H), 7.27 (d, $H_{6,6'}$, 4H), 2.16 (s, H_8, 6H), 2.22–2.21 (m, Hα, 4H), 1.81–1.78 (m, H_β, 4H), 1.49–1.47 (m, H_γ, 4H), 0.96 (t, H_δ, 6H). ^{13}C NMR ($CDCl_3$, ppm): 178.3 (C-1), 127.74 (C-2), 134.5 (C-3), 127.0 (C-4), 129.1 (C-5), 115.4 (C-6), 164.2 (C-7), 14.4 (C-8), 21.4 (C-α), 25.4 (C-β), 27.0 (C-γ), 13.6 (C-δ).

*2.2.5. Dioctyltin(IV) [bis(3-(4-flourophenyl)-2-methylacrylate)] (**3**)*

Compound **3** was prepared by using ligand acid, R/COOH (0.54 g, 3.0 mmol) and dioctyltin(IV) oxide (0.54 g, 1.5 mmol). The reactant mixture was suspended in 100 mL of dry toluene in a round bottom flask (250 mL), equipped with a Dean–Stark apparatus. The mixture was refluxed for 10 h and water formed during the condensation reaction was removed at regular intervals. The resultant clear solution obtained, was cooled to room temperature and solvent was removed under reduced pressure. The solid obtained was recrystallized from chloroform and *n*-hexane (4:1) mixture. Yield: (0.66 g, 68%). M.p. 150–151 °C. IR (cm^{-1}): 1508 $\nu(OCO)_{asym}$, 1366 $\nu(OCO)_{sym}$, ($\Delta\nu$ = 142 cm^{-1}), 532 ν(Sn–C), 461 ν(Sn–O). ^{1}H NMR ($CDCl_3$, ppm): 7.84 (s, H_3, 2H), 7.08 (d, $H_{5,5'}$, 4H), 7.53 (d, $H_{6,6'}$, 4H), 2.18 (s, H_8, 6H), 1.76–1.41 (bs, $H_{\alpha,\beta}$, 4H), 1.28–1.26 (bs, $H_{\gamma-\gamma'}$, 8H), 0.84 (t, $H_{\delta'}$, 6H). ^{13}C NMR ($CDCl_3$, ppm): 178.0 (C-1), 126.0 (C-2), 139.2 (C-3), 132.4 (C-4), 131.6 (C-5), 115.4 (C-6), 160.9 (C-7), 14.4 (C-8), 25.7 (C-α), 24.6 (C-β), 33.3 (C-γ), 31.8 (C-δ), 29.2 (C-α′), 29.1 (C-β′), 22.7 (C-γ′), 14.4 (C-δ′).

*2.2.6. Trimethyltin(IV) 3-(4-flourophenyl)-2-methylacrylate (**4**)*

Compound **4** was prepared in the same way as **1**, using R/COONa (0.2 g, 1.0 mmol) and trimethyltin(IV) chloride (0.41 g, 1.0 mmol) in 1:1 molar ratio. The product was recrystallized from chloroform and *n*-hexane (4:1) mixture. Yield: (0.51 g, 72%). M.p. 143–145 °C. IR (cm^{-1}): 1573 $\nu(OCO)_{asym}$, 1403 $\nu(OCO)_{sym}$, ($\Delta\nu$ = 170 cm^{-1}), 528 ν(Sn–C), 463 ν(Sn–O). ^{1}H NMR ($CDCl_3$, ppm): 7.67 (s, H_3, H), 7.42 (d, $H_{5,5'}$, 2H), 7.05 (d, $H_{6,6'}$, 2H), 2.11 (s, H_8, 3H), 0.52 (s H_α, 9H) $^2J(^{119/117}Sn–^1H)$ = [58/56 Hz]. ^{13}C NMR ($CDCl_3$, ppm): 173.8 (C-1), 132.0 (C-2), 137.2 (C-3), 129.7 (C-4), 131.0 (C-5), 115.2 (C-6), 160.6 (C-7), 14.6 (C-8), −4.93 (C-α), $^1J(^{119/117}Sn–C)$ = [388/379 Hz].

*2.2.7. Tributyltin(IV) 3-(4-flourophenyl)-2-methylacrylate (**5**)*

Compound **5** was prepared in the same way as **1**, using R/COONa (0.4 g, 2.0 mmol) and tributyltin(IV) chloride (0.64 g, 2.0 mmol) in 1:1 molar ratio. The product was recrystallized from chloroform and *n*-hexane (4:1) mixture. Yield: (0.68 g, 74%). M.p. 135–136 °C. IR (cm^{-1}): 1507 $\nu(OCO)_{asym}$, 1312 $\nu(OCO)_{sym}$, ($\Delta\nu$ = 195 cm^{-1}), 524 ν(Sn–C), 449 ν(Sn–O). ^{1}H NMR ($CDCl_3$, ppm): 7.66 (s, H_3, H), 7.38 (d, $H_{5,5'}$, 2H), 7.05 (d, $H_{6,6'}$, 2H), 2.11 (s, H_8, 3H), 1.75–1.63 (m, Hα, 6H), 1.45–1.40 (m, H_β, 6H), 1.37–1.31 (m, Hγ, 6H), 0.92 (t, H_δ, 9H). ^{13}C NMR ($CDCl_3$): 173.6 (C-1), 125.3 (C-2), 136.7 (C-3), 132.7 (C-4), 131.3 (C-5), 115.2 (C-6), 160.6 (C-7), 14.3 (C-8), 16.5 (C-α), 21.4 (C-β), 25.3 (C-γ), 13.7 (C-δ).

*2.2.8. Triphenyltin(IV) 3-(4-flourophenyl)-2-methylacrylate (**6**)*

Compound **6** was prepared in the same way as **1**, using R/COONa (0.5 g, 2.5 mmol) triphenyltin(IV) chloride (0.95 g, 2.5 mmol) in 1:1 molar ratio. The product was recrystallized from chloroform and *n*-hexane (4:1) mixture. Yield: (0.87 g, 67%). M.p. 139–140 °C. IR (cm^{-1}): 1582 $\nu(OCO)_{asym}$, 1392 $\nu(OCO)_{sym}$, ($\Delta\nu$ = 190 cm^{-1}), 536 ν(Sn–C), 441 ν(Sn–O). ^{1}H NMR ($CDCl_3$, ppm): 7.63 (s, H_3, H), 7.42 (d, $H_{5,5'}$, 2H), 7.12 (d, $H_{6,6'}$, 2H), 2.13 (s, H_8, 3H), 7.75–7.71 (H_β, H_γ, H_δ 15H). ^{13}C NMR ($CDCl_3$, ppm): 171.5 (C-1) 129.3 (C-2), 137.5 (C-3), 132.4 (C-4), 131.5 (C-5), 115.2 (C-6), 160.6 (C-7), 14.5 (C-8), 140.0 (C-α), 137.5 (C-β), 128.5 (C-γ), 129.4 (C-δ).

2.3. DNA interaction studies by UV–visible spectroscopy

0.2 g of SS-DNA (salmon sperm-DNA) was dissolved in 100 mL of double deionized water and kept at 4 °C for 2 days. Solutions of DNA in 20 mM Tris–HCl (pH 7.4) gave the ratio of UV absorbance at 260 and 280 nm, (A_{260}/A_{280}) of 1.86 indicating that the DNA is sufficiently free from protein [35]. The DNA concentration was determined via absorption spectroscopy using the molar absorption coefficient of 6600 M^{-1} cm^{-1} at 260 nm [36], and was found as 1.86 × 10^{-4} M. From this stock solution 13, 26, 39, 52 and 65 μM working solutions were prepared by dilution method. The complexes were dissolved in 10% DMSO at a concentration of 4 × 10^{-5} M. The UV absorption titrations were performed by keeping the complexes concentration fixed while varying the concentration of DNA. Equivalent solutions of DNA were added to the complex and reference solutions to eliminate the absorbance of DNA itself. Compound–DNA solutions were allowed to incubate for 30 min at ambient temperature before measurements were made. Absorption spectra were recorded using cuvettes of 1 cm path length.

2.4. Viscosity measurements

Viscosity measurements were carried out using Ubbelohde viscometer at ambient temperature of 23 ± 1 °C. Flow time was measured with a digital stopwatch. Each sample was measured three times and an average flow time was calculated. Data were presented as relative viscosity, $(\eta/\eta_o)^{1/3}$, vs binding ratio ([compound]/[DNA]) where η is the viscosity of DNA in the

presence of complex and η_o is the viscosity of DNA alone. Viscosity values were calculated from the observed flow time of DNA containing solution (t_o), $\eta = t - t_o$ [37].

2.5. Antibacterial studies

The synthesized ligand and its organotin(IV) complexes were tested against six bacterial strains; two Gram-positive (*Micrococcus luteus* and *Staphylococcus aureus*) and four Gram-negative (*Escherichia coli*, *Enterobacter aerogenes*, *Bordetella bronchiseptica* and *Klebsiella pneumoniae*). The agar well-diffusion method was used for the determination of antibacterial activity [37,38]. Broth culture (0.75 mL) containing ca. 10^6 colony forming units (CFU) per mL of the test strain was added to 75 mL of nutrient agar medium at 45 °C, mixed well, and then poured into a 14 cm sterile petri plate. The media was allowed to solidify, and 8 mm wells were dug with a sterile metallic borer. Then a DMSO solution of test sample (100 μL) at 1 mg/mL was added to the respective wells. DMSO served as negative control, and the standard antibacterial drugs *Roxithromycin* (1 mg mL^{-1}) and *Cefixime* (1 mg mL^{-1}) were used as positive control. Triplicate plates of each bacterial strain were prepared which were incubated aerobically at 37 °C for 24 h. The activity was determined by measuring the diameter of zone showing complete inhibition (mm).

2.6. Antifungal studies

Antifungal activity against five fungal strains (*Fusarium moniliformis*, *Aspergillus niger*, *Fusarium solani*, *Mucor species* and *Aspergillus fumigatus*) was determined by using Agar tube dilution method [39]. Screw caped test tubes containing Sabouraud dextrose agar (SDA) medium (4 mL) were autoclaved at 121 °C for 15 min. Tubes were allowed to cool at 50 °C and non solidified SDA was loaded with 66.6 μL of compound from the stock solution (12 mg mL^{-1} in DMSO) to make 200 μg mL^{-1} final concentration. Tubes were then allowed to solidify in slanting position at room temperature. Each tube was inoculated with 4 mm diameter piece of inoculum from seven days old fungal culture. The media supplemented with DMSO and *Turbinafine* (200 μg mL^{-1}) were used as negative and positive control, respectively. The tubes were incubated at 28 °C for 7 days and growth was determined by measuring linear growth (mm). The growth inhibition was calculated with reference to growth in vehicle control using the following equation.

$$\%\ \text{Growth inhibition} = 100 - \left(\frac{\text{Linear growth in test sample (mm)}}{\text{Linear growth in control (mm)}} \times 100\right)$$

2.7. Cytotoxic studies

Cytotoxicity was studied by the brine-shrimp lethality assay method [37,38]. Brine-shrimp (*Artemia salina*) eggs were hatched in artificial sea water (3.8 g sea salt L^{-1}) at ambient temperature of 23 ± 1 °C. After two days these shrimps were transferred to vials containing 5 mL of artificial sea water (10 shrimps per vial) with 10, 100 and 1000 μg mL^{-1} final concentrations of each compound taken from their stock solutions of 12 mg mL^{-1} in DMSO. After 24 h, number of surviving shrimps were counted. Data was analyzed with a Biostat 2009 computer programme (Probit analysis) to determine LD_{50} values.

2.8. Anti-tumor studies

The ligand **HL** and organotin(IV) carboxylates complexes **1**–**6** were screened for anti-tumor activity using crown gall tumor inhibition assay (potato disc assay) [40] using *Agrobacterium tumefaciens* (strain At10). *A. tumefaciens* cause Crown gall due to its Ti (tumor inducing) plasmid which is a neoplasmic disease of plants [40]. Vincristine was used as reference drug.

2.9. Catalytic experiment

Transesterification of rocket seed oil was carried out using triorganotin (IV) carboxylate catalysts in molar ratio of 400:100:1 of methanol, oil and catalyst. 0.01 mol rocket seed oil was transesterified using 0.04 mol methanol and 0.1 mmol catalyst in a 100 mL two neck round bottom flask equipped with reflux condenser, magnetic stirrer, thermometer and sampling outlet. Before the reaction, the triorganotin catalyst was solubilized in 0.5 mL chloroform. The reaction mixture was refluxed and stirred with a constant speed of 600 rpm. The sample was taken after 1,8,16 and 24 h and was analyzed by ^{1}H NMR to check the % age conversion of oil into biodiesel.

3. Results and discussion

3.1. Syntheses of complexes *1*–*6*

Diorganotin dichloride with NaL in 1:2, triorganotin chloride with NaL in 1:1 and R_2SnO with HL in 1:2 molar ratios give complexes according to the following equations

$$R_2SnCl_2 + 2NaL \rightarrow R_2SnL_2 + 2NaCl \quad (1)$$
$$R = CH_3(\mathbf{1}), n\text{–}C_4H_9(\mathbf{2}),$$

$$R_3SnCl + NaL \rightarrow R_3SnL + NaCl \quad (2)$$
$$R = CH_3(\mathbf{4}),\ n\text{–}C_4H_9(\mathbf{5}), C_6H_5(\mathbf{6})$$

$$R_2SnO + 2HL \rightarrow R_2SnL_2 + H_2O \quad (3) \quad R = n\text{–}C_8H_{17}(\mathbf{3})$$

3.2. FT-IR analysis

IR spectra of all the complexes (**1**–**6**) were analyzed in the range 4000–400 cm^{-1} and used to identify binding mode of COO^- moiety with Sn atom [41]. In the IR spectra of all complexes, the appearance of a new Sn–O vibration in the region 436–478 cm^{-1} indicated the deprotonation of the ligand upon coordination with di and triorganotin(IV) moiety via two oxygen atoms of the COO^- group [42,43]. Bands in the range of 515–586 cm^{-1} indicate the presence of Sn–C bonds. The $\Delta\nu$ difference between $\nu_{asym}(COO)^-$ and $\nu_{sym}(COO)^-$ is important to find out the binding mode of COO^- moiety with Sn atom. According to literature, $\Delta\nu$ greater than 250 cm^{-1} shows a monodentate while a value less than 250 cm^{-1} shows bidentate binding mode of COO^- moiety with Sn atom. Moreover a $\Delta\nu$ value between 150 and 250 cm^{-1} indicates a bridging behavior while a value less than 150 cm^{-1} exhibits

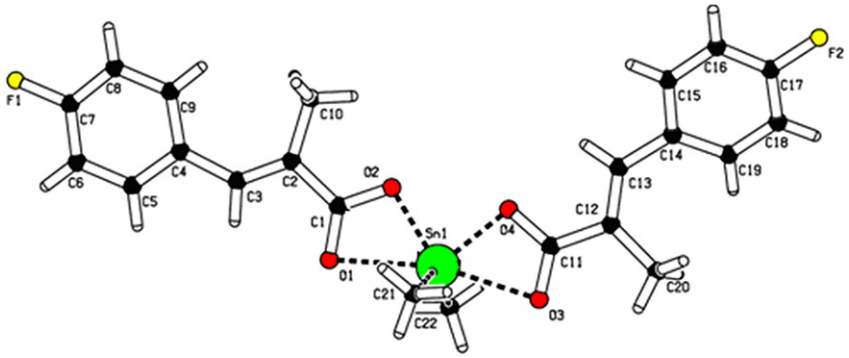

Fig. 1. Platon drawing of complex **1** with atomic numbering scheme.

a chelate structure [41]. In the present study, the complexes **1**–**3** exhibit chelating behavior while **4**–**6** show a bridging mode of coordination in solid state. These findings are well matched with X-ray crystal structures of complexes **1** and **4**.

3.3. NMR studies

3.3.1. ^{1}H NMR spectra

The ^{1}H NMR spectra represent the integration and multiplicities of all the protons in the ligand and in **1**–**6** complexes. The expected ppm values of aliphatic and aromatic protons showed good matching. The coordination of COO^{-} moiety with Sn atom was confirmed by disappearance of acid proton signal at 11.32 ppm and the formation of Sn–O bond [44,45]. The structural information was obtained by the coupling constant ^{2}J [$^{119}Sn/^{117}Sn$, ^{1}H]. The ^{2}J [$^{119}Sn/^{117}Sn$, ^{1}H] coupling constant value of 83/81 Hz, indicates six co-ordination behavior having octahedral geometry while ^{2}J [$^{119}Sn/^{117}Sn$, ^{1}H] of 58/56 Hz, indicates four coordination behavior having tetrahedral geometry [46–48] in solution. In ^{1}H NMR of compound **1** and **4**, the ^{2}J [$^{119}Sn/^{117}Sn$, ^{1}H] values are 83/80 and 58/56 Hz, indicating six and four coordination behavior in solution, respectively.

3.3.2. ^{13}C NMR spectra

In ^{13}C NMR, the different R (Me, *n*-But, *n*-Oct, Ph) groups attached to Sn atom gave signals in the expected region. The ^{1}J [$^{119}Sn/^{117}Sn$, ^{13}C] coupling constant for compound **1** and **4** are 570 and 378 Hz, which indicate six and four coordination behavior in solution, respectively.

3.4. Crystal structure of complex *1* and *4*

The structure of complex **1** is shown in Fig. 1. The crystal data, selected bond lengths and bond angles of complex **1** are listed in Tables 1 and 2. The carboxylate moiety COO^{-} of ligand is bonded as anisobidentate mode with two shorter bonds (Sn1–O2 and Sn1–O4) and two longer bonds (Sn1–O1, Sn1–O3) in asymmetric way as depicted in Table 2. The geometry at the central Sn atom is skew-trapezoidal in which the basal plane is defined by four oxygen atoms derived from the two chelating carboxylate ligands whereas the remaining two positions are occupied by two methyl groups. The longer Sn–O distances are significantly less than the sum of the van der Waal's radii (3.68 Å) [49], and the coordination number of Sn is unambiguously assigned as six. The methyl groups do not occupy the exact axial positions as a result C–Sn–C angle is 134.99(9)° which falls in the range (122.6–156.9) for skew-trapezoidal geometry [50,51]. The asymmetric mode of coordination of the carboxylate ligands is further confirmed by unequal C–O bond distances; O1–C1 = 1.241(2) Å, O2–C1 = 1.300(2) Å and O3–C11 = 1.240(3) Å, O4-C11 = 1.299(2) Å as depicted in Table 2. The geometry, bond lengths (Sn1–O1, Sn1–O2, Sn1–O3, Sn1–O4) and angles (O2–Sn1–O1, O2–Sn1–O3, O3–Sn1–O1, O4–Sn1–O1, O4–Sn1–O2, O4–Sn1–O3) are comparable with literature values [52,53].

The structure of complex **4** is shown in Fig. 2. The crystal data, selected bond length and bond angles of complex **4** are listed in Tables 1 and 3. The complex **4** showed polymeric structure with trigonal bipyramidal geometry. The carboxylate oxygen make zig zag chain with anti–syn configuration. The C–Sn–C angles are in the range 112.0(2)–124.5(2)°. The axial positions are occupied by the two oxygen atoms of bridging carboxylate ligands having O–Sn–O angle 172.30(4)°. Thus carboxylate ligand bridges the two symmetry related Sn atoms and gives rise to the unequal Sn–O bond distances which are reflected in the associated C–O bond lengths, the longer C–O bond is involved in the shorter Sn–O interaction and vice versa. These bond lengths are in accordance with the reported triorganotin(IV) carboxylates [54,55]. The polymeric bridging behavior is comparable with literature [49,50].

Table 1
Crystal data and structure refinement parameters for complexes **1** and **4**.

Compound	**1**	**4**
Chemical formula	$C_{22}H_{22}F_2O_4Sn$	$C_{13}H_{17}FO_2Sn$
Formula mass (g mol^{-1})	507.09	342.96
Crystal system	Monoclinic	Monoclinic
Space group	*P* 21/*c*	*P* 21/*c*
Unit cell dimensions		
a (Å)	9.9206(3)	6.7977(2)
b (Å)	17.0397(5)	9.7882(3)
c (Å)	13.3651(3)	21.0089(7)
α (°)	90.00	90.00
β (°)	109.7080(10)	97.884(2)
γ (°)	90.00	90.00
Volume (Å^3)	2126.95(10)	1384.66(7)
Z	4	4
Temperature (K)	296(2)	296(2)
Density (calculated) (g cm^{-3})	1.584	1.645
Absorption coefficient (mm^{-1})	1.243	1.845
F(000)	1016	680
Radiation (A^0) (Mo K/*α*)	0.71073	0.71073
Index ranges	*h*: −11 → 11; *k*: −20 → 20; *l*: −15 → 16	*h*: −8 → 8; *k*: −11 → 12; *l*: −25 → 25
θ (°) Min Max	2.18–25.24	2.30–26.00
Total reflections	3839	2718
Data/restraints/parameters	3839/0/267	2718/0/159
R_{all}, R_{gt}	0.0222, 0.0197	0.0377, 0.0352
*WR*ref, *WR*gt	0.0528, 0.0506	0.0884, 0.0875
Goodness-of-fit	1.053	1.287

Table 2
Selected bond lengths (Å) and bond angles (°) of complex **1**.

Bond lengths (Å)			
Sn–C21	2.101(2)	Sn1–O4	2.0937(12)
Sn–C22	2.087(2)	O1–C1	1.241(2)
Sn1–O1	2.5352(15)	O2–C1	1.300(2)
Sn1–O2	2.0937(13)	O3–C11	1.240(3)
Sn1–O3	2.4846(15)	O4–C11	1.299(2)
Bond angles (°)			
O2–Sn1–O1	55.47(5)	C22–Sn1–O1	88.64(7)
O2–Sn1–O3	138.82(5)	C22–Sn1–O3	85.61(7)
O3–Sn1–O1	165.69(5)	C22–Sn1–O4	107.15(7)
O4–Sn1–O1	138.21(5)	C21–Sn1–O1	86.59(7)
O4–Sn1–O2	82.75(5)	C21–Sn1–O3	88.23(8)
O4–Sn1–O3	56.09(5)	C22–Sn1–C21	134.99(9)
O4–Sn1–C21	105.90(8)		

3.5. DNA binding studies

The mode of interaction of organotin(IV) carboxylates with DNA was determined by UV–visible absorption spectroscopy which is one of the useful techniques for this purpose [56–58]. The comparison of absorbance and shift in the wavelength of ligand and complexes with and without SS-DNA give the idea about the interaction of ligand or metal complexes with DNA [59].

The absorption spectra of ligand **HL** and organotin(IV) carboxylates **1** and **4** in the absence and presence of SS-DNA (salmon sperm) have been recorded at different concentration of DNA by keeping concentration of ligand **HL** and organotin(IV) carboxylates constant. There exists a single band in the absorption spectrum at 266.80 nm (**HL**), 260 nm (**1**) and 260.50 nm (**4**). The UV studies of ligand **HL** showed (Fig. 3) hyperchromic effect. This suggests that **HL** binds with DNA double helix by hydrogen bonding between the ligand and the base pairs in DNA typically to N3 of adenine and O2 of thymine [60] resulting in bathochromism or classical electrostatic interaction due to protonated ligand [61]. While the organotin(IV) carboxylates **1** and **4** (Figs. 4 and 5) showed significant hypochromic effect. This suggest mainly intercalation as well as by groove mode of binding which may be due to presence of phenyl group of ligand that facilitates the interaction with DNA [56,62]. After 24 h, the spectrum was again taken and obtained the same results which confirm the stability of drug–DNA complex.

The intrinsic binding constant K of the ligand **HL** and organotin(IV) carboxylates **1** and **4** were calculated in order to compare binding strengths of ligand–DNA and complex–DNA by using Benesi–Hildebrand equation [40]:

$$\frac{A_0}{A-A_0} = \frac{\varepsilon_G}{\varepsilon_{H-G}-\varepsilon_G} + \frac{\varepsilon_G}{\varepsilon_{H-G}-\varepsilon_G} \times \frac{1}{K[DNA]}$$

where K is the binding constant, A_0 and A are the absorbance of the drug and its complex with DNA, and ε_G and ε_{H-G} are the absorption coefficients of the drug and the drug–DNA complex, respectively. The binding constants were obtained from the intercept-to-slope ratios of $A_0/(A - A_0)$ vs. 1/[DNA] plots. The binding constants were found to be 3.5×10^4 M^{-1} (**HL**), 6.37×10^3 M^{-1} (**1**) and 5.0×10^4 M^{-1} (**4**).

The Gibb's free energy (ΔG) of the ligand **HL** and organotin(IV) carboxylates **1** and **4** were determined by using the following equation:

$$\Delta G = -RT \ \ln K$$

where R is general gas constant (8.314 J K^{-1} mol^{-1}) and T is the temperature (298 K). The Gibb's free energies were found −11.3 (**HL**), −9.43 (**1**), and −11.64 kJ mol^{-1} (**4**), indicating the interaction of the compounds with DNA is a spontaneous process.

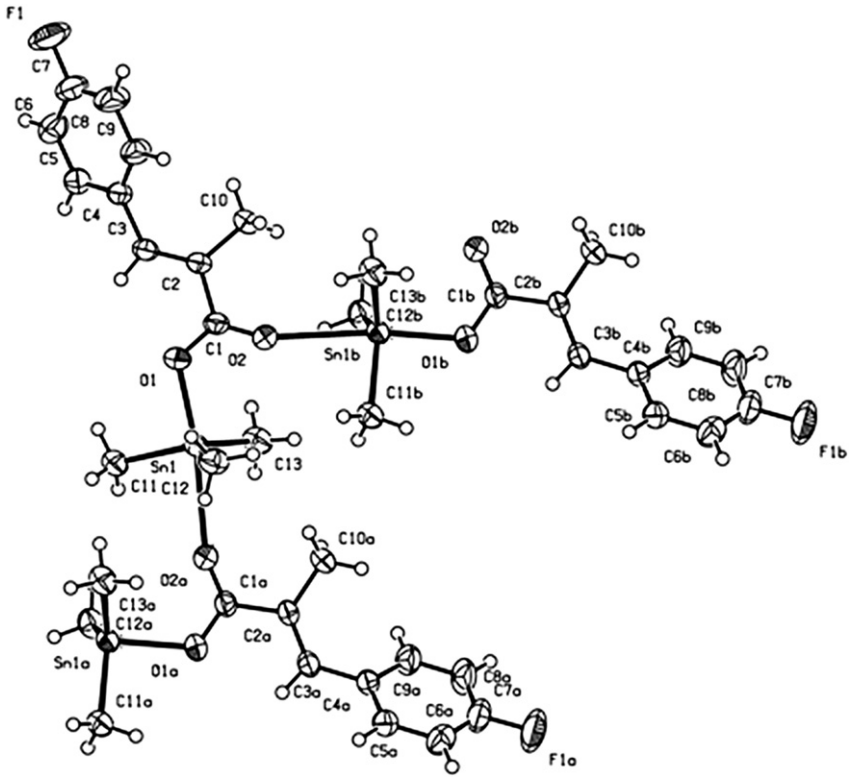

Fig. 2. Platon drawing of complex **4** with atomic numbering scheme.

Table 3
Selected bond lengths (Å) and bond angles (°) of complex **4**.

Bond lengths (Å)			
Sn–C11	2.125(5)	O1–C1	1.297(6)
Sn–C12	2.109(5)	O2–C1	1.229(6)
Sn–C13	2.125(5)	Sn1–O1	2.116(3)
Bond angles (°)			
O1–Sn–O2	172.30(4)	C11–Sn–C12	119.9(2)
O1–Sn–C11	92.19(18)	C12–Sn–C13	124.5(2)
O1–Sn–C12	97.50(19)	C11–Sn–C113	112.0(2)
O1–Sn1–C13	99.21(19)	C1–O1–Sn1	120.2(3)

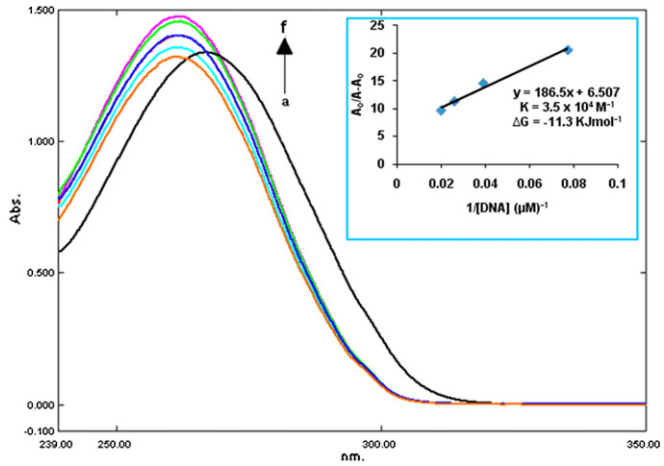

Fig. 3. Absorption spectra of 0.04 mM **HL** in the absence (a) and presence of 13 μM (b), 26 μM (c), 39 μM (d), 52 μM (e), 65 μM (f) DNA. The arrow direction indicates increasing concentrations of DNA. Inside graph is the plot of $A_o/(A - A_o)$ vs. 1/[DNA] for the determination of binding constant and Gibb's free energy of **HL** − DNA adduct.

3.6. Viscosity measurements

To further clarify the binding modes of the **HL** and its representative complexes **1** and **4** with DNA, viscosity measurements were carried out. Hydrodynamic measurements that are sensitive to length change (i.e., viscosity) are regarded as the least ambiguous and the most critical tests of the binding model in solution. A classical intercalation model resulted in the lengthening of the DNA helix as the base pairs were separated to accommodate the binding complex, leading to an increase in DNA viscosity [63]. There is a marked effect of **HL**, **1** and **4** on the viscosity of SS-DNA as shown in Fig. 6. With the increase in the concentration of **HL**, the relative viscosity of **HL**–DNA mixture remains almost constant and then starts increasing with further increase in **HL** concentration which indicates that groove binding also contribute to some extent. After that the increase in the effective length of DNA supports that **HL** binds through intercalation mode but with different affinity, i.e., also show some affinity for binding with grooves of DNA through hydrogen bonding. However, strong binding is presumably due to intercalation with DNA [64]. The viscosity of mixture of complexes **1** and **4** with SS-DNA was increased gradually with the increase in the concentration of the complexes, indicating intercalative interaction mode of theses complexes with SS-DNA [37].

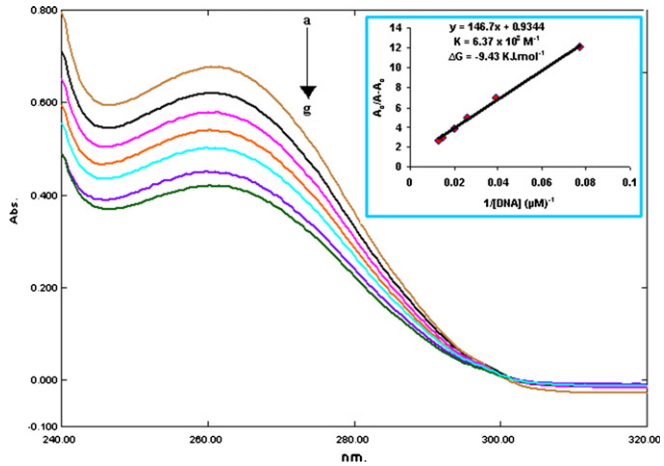

Fig. 4. Absorption spectra of 0.04 mM compound **1** in the absence (a) and presence of 13 μM (b), 26 μM (c), 39 μM (d), 52 μM (e), 65 μM (f) and 78 μM (g) DNA. The arrow direction indicates increasing concentrations of DNA. Inside graph is the plot of $A_o/(A - A_o)$ vs. 1/[DNA] for the determination of binding constant and Gibb's free energy of complex **4** − DNA adduct.

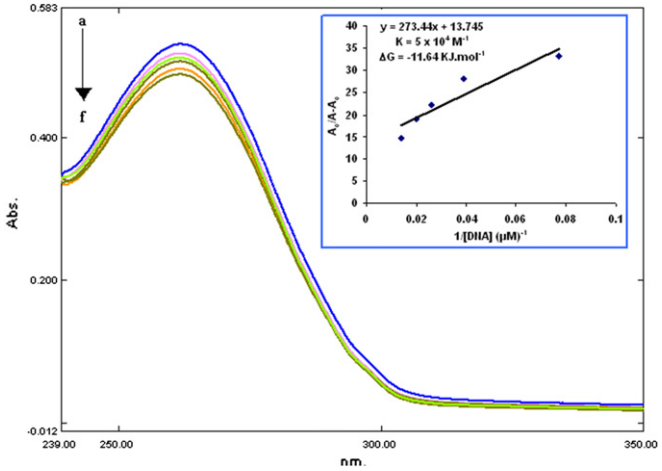

Fig. 5. Absorption spectra of 0.04 mM compound 4 in the absence (a) and presence of 13 μM (b), 26 μM (c), 39 μM (d), 52 μM (e) and 65 μM (f) DNA. The arrow direction indicates increasing concentrations of DNA. Inside graph is the plot of $A_o/(A - A_o)$ vs. 1/[DNA] for the determination of binding constant and Gibb's free energy of complex **1** − DNA adduct.

3.7. Biological studies

3.7.1. Antibacterial studies

In vitro biological screening tests of the synthesized ligand **HL** and its organotin(IV) complexes (**1**–**6**) were carried out for antibacterial activity. The experiment was performed in triplicate by

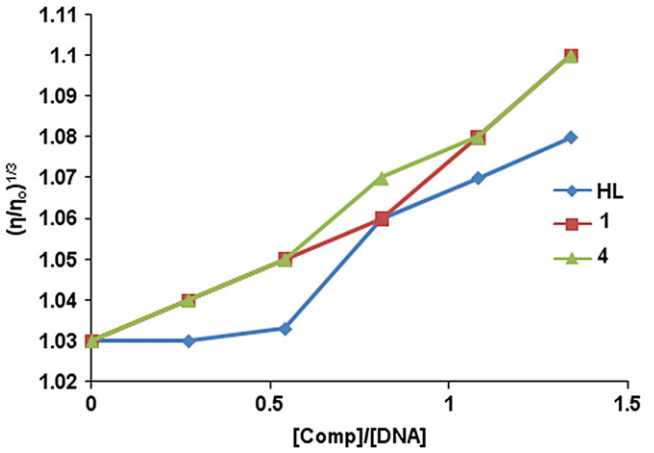

Fig. 6. Effects of increasing concentration of **HL**, complexes **1** and **4** on relative viscosity of SS-DNA at 25 ± 0.1 °C. [DNA] = 1.86 × 10^{-4} M.

Table 4
Antibacterial data of **HL** and its organotin(IV) complexes (**1**–**6**).

Compound	Average zone of inhibition (mm)					
	Staphylococcus aureus	*Escherichia coli*	*Bordetella bronchiseptica*	*Pseudomonas aeruginosa*	*Micrococcus luteus*	*Klebsiella pneumoniae*
HL	0	15	0	0	15	0
1	15	14	15	0	14	10
2	0	20	0	0	13	11
3	0	20	0	0	0	0
4	22	20	25	18	20	15
5	22	25	24	17	18	12
6	30	17	35	15	25	12
Cefixime	22	25	20	23	25	22
Roxithromycin	25	25	25	25	30	30

Concentration: 1 mg/mL of DMSO. Reference drugs, *Roxythromycin* and *Cefixime* 1 mg/mL.

agar well-diffusion method. *Roxithromycin* and *Cefixime* were used as positive control. The results are shown in Table 4. Criteria for activity is based on zone of inhibition (mm); inhibition zone more than 20 mm shows significant activity, for 18–20 mm inhibition activity is good, 15–17 mm is low, and below 11–14 mm is non-significant [37]. The antibacterial study demonstrates that all compounds except ligand **HL** and complex **3** have activity toward tested bacteria. Complex **6**, exhibited greater activity against two pathogenic strains, *S. aureus* and *B. bronchiseptica* than both standard drugs while good activity against *M. luteus*. The complexes **4** and **5** showed significant activity against four strains *S. aureus*, *E. coli*, *B. bronchiseptica* and *M. luteus*, whereas the activity exhibited against *B. bronchiseptica* is better than *Cefixime*, used as positive control. Complex **1** showed non significant to low activity against all pathogenic strains. Complex **2** showed non significant to good activity against all tested strains.

3.7.2. Antifungal studies

The ligand **HL** and its organotin(IV) complexes (**1**–**6**) were also screened for antifungal activity against five fungal strains (*Aspergillus flavus*, *A. niger*, *A. fumigatus*, *F. solani* and *M. species*) by using Agar tube dilution method. The results are shown in Table 5. *Terbinafine* was used as standard drug in this assay. Criteria for activity is based on percent growth inhibition; more than 70% growth inhibition was considered as significant activity, 60–70% inhibition activity as good, 50–60% inhibition activity as moderate while below 50% inhibition activity was considered as non-significant. The results show that the synthesized organotin(IV) complexes in general have more activity than the ligand **HL** except for complexes **1** and **3** which exhibited non-significant against all the tested strains. Complexes **4** and **5** showed 100% growth inhibition against all tested fungal strains like the reference drug used. The complex **5** exhibited 100% growth inhibition against three fungal strains, *A. niger*, *A. fumigatus*, and *M. species* while complex **2** exhibited significant inhibiting activity against three fungal strains, *A. flavus*, *A. niger*, and *F. solani*.

Significantly higher antimicrobial activity of the reported complexes as compared to organotin carboxylates could probably be due to the presence of highly polar flouro group on benzene ring which offers greater interaction with the cell constituents of the microorganisms [65].

Table 5
Antifungal activity data of **HL** and its organotin(IV) complexes (**1**–**6**).

Compound	Mean value of percent growth inhibition (%)				
	Aspergillus flavus	*Aspergillus niger*	*Aspergillus fumigatus*	*Fusarium solani*	*Mucor species*
HL	40	62.5	0	0	55
1	10	20	10	0	40
2	77	85	0	85	47.5
3	0	20	45	10	10
4	100	100	100	100	100
5	40	100	100	45	100
6	100	100	100	100	100
Terbinafine	100	100	100	100	100

In vitro agar tube dilution method, concentration: 200 μg/mL of DMSO. % Inhibition of fungal growth = 100 − gt/gc × 100. Gt = linear growth in test (mm) and gc = linear growth in vehicle control (mm).

3.7.3. Cytotoxic studies

The cytotoxicities of ligand **HL** and its organotin(IV) complexes (**1**–**6**) were studied *in vitro* against the brine-shrimp lethality method by using reference drug MS-222 (*Tricaine methanesulfonate*) and the results are summarized in Table 6. The data is based on mean value of 2 replicates each of 10, 100 and 1000 μg mL^{-1}. The LD_{50} data exhibited that ligand **HL** and all the tested organotin(IV) complexes are toxic having values in the range 0.108–46.31 μg mL^{-1} with reference having the value 4.3 μg mL^{-1}. Complexes **2**, **4**–**6** were proved to be most toxic as compared to tested compounds and reference drugs.

3.7.4. Anti-tumor studies

The anti-tumor activity of ligand **HL** and organotin(IV) complexes (**1**–**6**) was evaluated by crown gall tumor inhibition assay (potato disc assay) because the mechanism of tumor

Table 6
Cytotoxicity data of **HL** and its organotin(IV) complexes (**1**–**6**).

Compound	No. of shrimps killed out of 20 per dilution[a]			LD_{50}
	1000 μg mL^{-1}	100 μg mL^{-1}	10 μg mL^{-1}	
HL	20	17	0	13.01
1	20	11	5	46.31
2	20	18	15	1.81
3	20	18	5	22.08
4	20	20	20	–
5	20	20	20	–
6	20	19	18	0.108
Vehicle control	0	0	0	

[a] Against brine-shrimps (*in vitro*).

Table 7
Antitumor data of **HL** and its organotin(IV) complexes (**1**–**6**).

Compound no.	No. of tumors	No. of tumors/disc	% Inhibition
HL	27	2.3	69
1	4.0	0.4	95
2	15	1.7	77
3	25	2.1	72
4	3.0	0.3	96
5	2.0	0.2	97
6	0.0	0.0	100
Vincristine	0.0	0.0	100
Control	82	7.5	–

Table 8
% age conversion of triglycerides in rocket seed oil to FAMEs.

Catalyst	Time (h)	% Conversion
Me_3SnL (**4**)	1	0.0
	8	35.21
	16	65.73
	24	84.19
Bu_3SnL (**5**)	1	0.0
	8	21.56
	16	30.82
	24	53.73
Ph_3SnL (**6**)	1	0.0
	8	17.45
	16	29.34
	24	43.0
NaOH	1.5	88.49

induction is similar to that seen in animals. All the complexes showed significant levels of tumor inhibition, as shown in Table 7. The complexes **1**–**6** exhibited more activity than ligand **HL**. The complex **6** exhibited 100% anti-tumor activity. Moreover complexes **4**–**6** exhibited excellent activity than complexes **1**–**3** which is consistent to the earlier reports on organotin(IV) carboxylates [40]. The results showed the order **6** > **5** > **4** > **1** > **2** > **3**.

3.8. Catalytic activity of compounds *4*–*6*

The catalytic activity of triorganotin(IV) carboxylates **4**–**6** was investigated in a transesterification reaction on triglycerides in oil with methanol. The tin complexes are selected due to the Lewis acid character of tin. The tin atom has the property of coordination expansion which may play an important role in the catalytic activity of different substituted organotin compounds. The activation of carbonyl groups in triglycerides to increase the electrophilicity of the carbonyl carbon and a subsequent interaction with tin atom. Since Lewis acid catalysts can activate carbonyl groups, our interest was concentrated on metal complexes with fluorinated ligands, whose Lewis acidity may depend on the groups attached to metal (e.g. Sn) and nucleophilicity by fluorinated ligand.

The transesterification reaction was carried out in molar ratio of 400:100:1 (methanol, oil and catalyst) as reported in literature [30]. The conditions for experiments were not optimized and no attempt was made to remove the added catalyst from the reaction mixture. The sample was taken from the reaction mixture at regular interval of 1, 8, 16 and 24 h and was analyzed by ^{1}H NMR to calculate % age conversion of triglycerides into fatty acid methyl esters (FAMEs) [66,67]. The results are summarized in Table 8. The equation used to quantify the extent of transesterification was:

$$C = 100\frac{2A_{Me}}{3A_{CH_2}} \quad (4)$$

where

C = percentage conversion of triglycerides to corresponding methyl esters
A_{Me} = integration value of the methoxy protons of the methyl esters and
A_{CH_2} = integration value of α-methylene protons

All the experiments were carried out in the presence of ligand **HL** as catalyst but transesterification was not detected at all. The

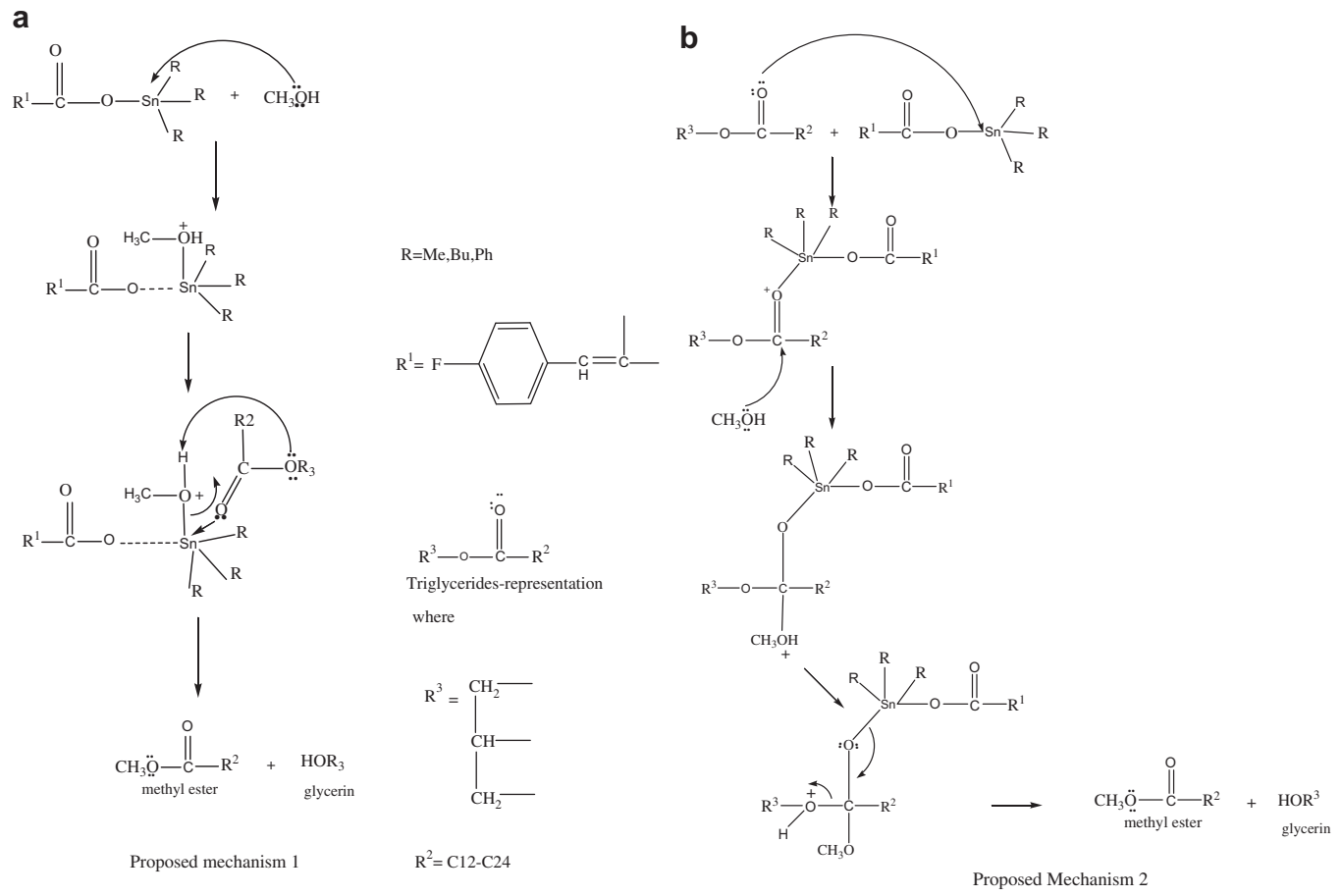

Fig. 7. a and b: Proposed mechanism for transesterification of triglycerides into fatty acid methyl esters (biodiesel).

catalytic activity of triorganotin(IV) carboxylates **4**–**6** was also compared with traditional base catalyst NaOH [68] using molar ratio of methanol, oil and catalyst 6:1:0.75. The results are summarized in Table 8. Although base catalyst gave high % age conversion in less time as compare to triorganotin(IV) carboxylates **4**–**6**, which work slowly and gave almost the same % age conversion (compound **4**) in 24 h but this research may open new ways to overcome the problems associated with use of base catalysts. The proposed mechanisms for the catalytic activity of organotin(IV) carboxylates is the Lewis acid character of tin atom [69–71] as in case of polyesterification and are shown in Fig. 7a–b). The Lewis acidity of Sn atom increase in the order, Me < Bu < Ph because methyl and butyl groups are electron donating while phenyl is electron withdrawing group [72,73]. The stronger the Lewis acidity, greater would be catalytic efficiency but in our studies catalytic performance is in reverse order which may be due to size of groups (Me, Bu, Ph) attached to Sn atom. As the group attached to Sn atom increase in size, the attack on the bulky triglycerides becomes difficult so Me_3SnL perform better than Bu_3SnL and Ph_3SnL.

4. Conclusion

Six organotin(IV) carboxylate complexes of 3-(4-flourophenyl)-2-methylacrylic acid were synthesized with the aim to develop new biologically active compounds. The complexes were characterized by FT-IR, NMR (^1H and ^{13}C) and X-ray crystallography. The interactions of ligand **HL** and complexes **1** and **4** were studied with SS-DNA using UV–visible spectroscopy and viscosity measurements. The results indicated intercalation mode of binding for complexes **1** and **4** while hydrogen bonding between the ligand and the base pairs in DNA or classical electrostatic interaction due to protonated ligand. The intrinsic binding constants K were found to be 3.5×10^4, 6.37×10^3 and 5.0×10^4 M^{-1} for **HL**, complexes **1** and **4**, respectively. The antimicrobial results showed that triorganotin(IV) carboxylates complexes **4**–**6** exhibit greater activity than diorganotin(IV) carboxylates complexes **1**–**3**. The cytotoxic studies revealed that complexes **4**–**6** were the most toxic as compared to tested compounds and reference drugs. The anti-tumor activities revealed that complex **6** has 100% inhibition while overall order is **6** > **5** > **4** > **1** > **2** > **3** > **HL**. The catalytic activity of compounds **4**–**6** was assessed for transesterification of rocket seed oil using methanol, oil, catalyst molar ratio of 400:100:1. The Me_3SnL exhibited good catalytic activity as compare to Bu_3SnL and Ph_3SnL which is reverse the order of Lewis acidity because groups (Me, Bu, Ph) attached to Sn atom play important role on attacking of bulky triglyceride molecule to the Sn center.

Acknowledgments

M. Tariq (Pin No. 074-0616-Ps4-099) is thankful to higher education commission of Pakistan for financial support during the present study.

Appendix A. Supplementary material

CCDC 891313 and 891312 for complexes **1** and **4**; contain the supplementary crystallographic data for this paper. These data can be obtained free of charge from The Cambridge Crystallographic Data Centre via deposit@ccdc.cam.ac.uk or http://www.ccdc.cam.ac.uk.

References

[1] M.I. Khan, M.K. Baloch, M. Ashfaq, S. Gul, J. Braz. Chem. Soc. 20 (2009) 341–347.
[2] L. Pellerito, L. Nagy, Coord. Chem. Rev. 224 (2002) 111–150.
[3] M.I. Khan, M.K. Baloch, M. Ashfaq, J. Organomet. Chem. 689 (2004) 3370–3378.
[4] Q. Li, M.F.C. Guedes da Silva, A.J.L. Pombeiro, J. Eur. Chem. 10 (2004) 1456–1462.
[5] X. Shang, X. Meng, E.C.B.A. Alegria, Q. Li, M.F.C. Guedes da Silva, M.L. Kuznetsov, A.J.L. Pombeiro, Inorg. Chem. 50 (2011) 8158–8167.
[6] E.R.T. Tiekink, Appl. Organomet. Chem. 5 (1991) 1–23.
[7] M. Hussain, M. Zaman, M. Hanif, S. Ali, M. Danish, J. Serb. Chem. Soc. 73 (2008) 179–187.
[8] A.G. Davies, Organotin Chemistry, second ed., Wiley-VCH Verlag GmbH & Co., Weinheim, 2004.
[9] P. Fierens, G.V.D. Dunghen, W. Segers, R.V. Elsuwe, React. Kinet. Lett. 85 (1978) 179–187.
[10] C.J. Evans, S. Karpel, J. Organomet. Chem. Libr. 16 (1985). Elsevier Science Publishers B.V., Nertherlands.
[11] S. Karpel, Tin and Its Uses 149 (1986) 1–6.
[12] F.W. van Der Weij, Macromol. Chem. Phys. 181 (1980) 2541–2548.
[13] D. Seyferth, T.C. Masterman, Appl. Organomet. Chem. 8 (1994) 335–350.
[14] A.A. Mahmoud, A.F. Shaaban, M.M. Azab, N.N. Messia, Eur. Poylm. J. 28 (1992) 555–559.
[15] J.R. Dharia, C.P. Pathak, G.N. Babu, S.K. Gupta, J. Polym. Sci. 26 (1988) 595–599.
[16] R. Gachter, H. Muller, Plastics Additives Handbook, Hanser Publisher, Munich, 1990, 281–287.
[17] J. Otera, Chem. Rev. 93 (1993) 1449–1470.
[18] J.K. Tsagatakis, N.A. Chaniotakis, K. Jurkschat, S. Damonun, P. Geerlings, A. Bouhdid, M. Gielen, I. Verbruggen, M. Biesemans, J.C. Martins, R. Willem, Helv. Chim. Acta 82 (1999) 531–542.
[19] C. Gaina, V. Gaina, M. Cristea, J. Inorg. Organomet. Polym. 19 (2009) 157–165.
[20] P. De Filippis, C. Giavarini, M. Scarsella, M. Sorrentino, J. Am. Oil Chem. Soc. 11 (1995) 1399–1404.
[21] H. Fukuda, A. Kendo, H.J. Nuda, Biosci. Bioeng. 92 (2001) 405–416.
[22] A. Srivastava, R. Prasad, Renew. Sustain. Energ. Rev. 4 (2000) 111–133.
[23] G. Labeckas, S. Slavonskas, Energ. Convers. Manag. 47 (2006) 1954–1967.
[24] U. Rashid, F. Anwar, Fuel 87 (2008) 265–273.
[25] N. Azcan, A. Danisman, Fuel 86 (2007) 2639–2644.
[26] L.C. Meher, M.G. Kulkarni, A.K. Dalai, S.N. Naik, Eur. J. Lipid Sci. Technol. 108 (2006) 3898–3978.
[27] M. Kim, S. Yan, S.O. Salley, K.Y.S. Ng, Biores. Technol. 101 (2010) 4409–4414.
[28] X. Liu, H. He, Y. Wang, S. Zhu, Catal. Commun. 8 (2007) 1107–1111.
[29] W. Xie, H. Peng, L. Chen, J. Mol. Catal. A Chem. 246 (2006) 24–32.
[30] F.R. Abreu, D.G. Lima, E.H. Hamu, S. Einloft, J.C. Rubin, A.Z. suarez, J. Am. Oil Chem. Soc. 80 (2003) 601–604.
[31] F.R. Abreu, D.G. Lima, E.H. Hamu, C. Wolf, P.A.Z. Suarez, J. Mol. Catal. A Chem. 209 (2004) 29–33.
[32] S. Einloft, T.O. Magalhaes, A. Donato, J. Dullis, R. Ligabue, Energy Fuel 22 (2008) 671–674.
[33] L. Angiolini, D. Caretti, L. Mazzocchetti, E. Salatelli, R. Willem, M. Biesemans, J. Organomet. Chem. 691 (2006) 1965–1972.
[34] D.D. Perrin, W.L.F. Armarego, Purification of Laboratory Chemicals, third ed., Pergamon Press, Berlin, Oxford, 2003.
[35] Y. Zhang, X. Wang, L. Ding, Nucleosides, Nucleotides and Nucleic Acids 30 (2011) 49–62.
[36] C.V. Sastri, D. Eswaramoorthy, L. Giribabu, B.G. Maiya, J. Inorg. Biochem. 94 (2003) 138–145.
[37] M. Sirajuddin, S. Ali, N.A. Shah, M.R. Khan, M.N. Tahir, Spectrochim. Acta Part A 94 (2012) 134–142.
[38] A. Rehman, M.I. Choudhary, W.J. Thomsen, Bioassay Techniques for Drug Development, Harwood Academic Publishers, Amsterdam, The Netherlands, 2001.
[39] B.N. Mayer, N.R. Ferrigni, J.E. Putnam, L.B. Jacobson, D.E. Nichols, J.L. Mclaughlin, Planta Med. 45 (1982) 31–34.
[40] M.S. Ahmad, M. Hussain, M. Hanif, S. Ali, B. Mirza, Molecules 12 (2007) 2348–2363.
[41] G. Eng, X. Song, A. Zapata, A.C. de Dios, L. Casabianca, R.D. Pike, J. Organomet. Chem. 692 (2007) 1398–1404.
[42] Q. Xie, Z. Yang, L. Jiang, Main Group Met. Chem. 19 (1996) 509–520.
[43] H.D. Yin, C.L. Ma, Y. Wang, H.X. Fang, J.X. Sao, Acta Chim. Sinica 60 (2002) 897–903.
[44] J. Li, G. Zhao, C. Xiong, Y. Ma, Synth. React. Inorg. Met. Org. Chem. 31 (2001) 85–93.
[45] S. Shahzadi, K. Shahid, S. Ali, M. Bakhtiar, Turk. J. Chem. 32 (2008) 333–353.
[46] F. Ahmad, M. Parvez, S. Ali, M. Mazhar, A. Munir, Synth. React. Inorg. Met. Org. Chem. 32 (2002) 665–687.
[47] M.M. Amini, A. Azadmeher, H.R. Khavsi, S.W. Ng, J. Organomet. Chem. 692 (2007) 3922–3930.
[48] K. Shahid, S. Ali, S. Shahzadi, A. Badshah, K.M. Khan, G.M. Maharvi, Synth. React. Inorg. Met. Org. Chem. 33 (2003) 1221–1235.
[49] E.R.T. Tiekink, Trends Organomet. Chem. 1 (1994) 71–116.
[50] S.W. Ng, C. Wei, V.G.K. Das, T.C.W. Mak, J. Organomet. Chem. 334 (1987) 295–305.
[51] S.G. Teoh, S.H. Ang, J.P. Declercq, Polyhedron 16 (1997) 3729–3733.
[52] M. Parvez, S. Ali, T. Masood, M. Mazhar, M. Danish, Acta Crystallogr. C53 (1997) 1211–1213.
[53] A. Ruzicka, L. Dostal, R. Jambor, V. Buchta, J. Brus, Appl. Organomet. Chem. 16 (2002) 315–322.

[54] C.L. Ma, Q.F. Zhang, R.F. Zhang, L.L. Qiu, J. Organomet. Chem. 690 (2005) 3033–3043.
[55] A.W. Addison, R.T. Nageswara, J. Reedijk, R.J. Van, G.C. Verschoor, J. Chem. Soc. Dalton Trans. 7 (1984) 1349–1356.
[56] K.S. Prasad, L.S. Kumar, K.B. Vinay, S.C. Shekar, B. Jayalakshmi, H.D. Revanasiddappa, Int. J. Chem. Res. 2 (2011) 1–6.
[57] G.N. Kalu Cerovi, D. Perez-Quintanilla, I. Sierra, S. Prashar, I. del Hierro, Z. Zizak, Z.D. Jurani, M. Fajardo, S. Gomez-Ruiz, J. Mater. Chem. 20 (2010) 806–814.
[58] O.R. Allen, A.L. Gott, J.A. Hartley, J.M. Hartley, R.J. Knox, P.C. McGowan, Dalton Trans. 43 (2007) 5082–5090.
[59] S. Tabassum, G.C. Sharma, F. Arjmand, A. Azam, Nanotechnology 21 (2010) 1–10.
[60] G.J. Chen, X. Qiao, P.Q. Qiao, G.J. Xu, J.Y. Xu, J.L. Tian, W. Gu, X. Liu, S.P. Yan, J. Inorg. Biochem. 105 (2011) 119–126.
[61] S. Gomez-Ruiz, J. Ceballos-Torres, S. Prashar, M. Fajardo, Z. Zizak, Z.D. Jurani, G.N. KaluCerovi, J. Organomet. Chem. 696 (2011) 3206–3213.
[62] N. Shahabadi, S. Mohammadi, R. Alizadeh, Bioinorg. Chem. Appl. 2011 (2011) 1–8.
[63] N. Shahabadi, S. Kashanian, F. Darabi, Eur. J. Med. Chem. 45 (2010) 4239–4245.
[64] F.J. Huoa, C.X. Yin, Y.B. Wu, P. Yang, Russ. J. Inorg. Chem. 55 (2010) 1087–1093.
[65] Z. Rehman, N. Muhammad, A. Shah, S. Ali, I.S. Butler, A. Meetsma, J. Coord. Chem. 65 (2012) 3238–3253.
[66] G. Gelbard, O. Bres, R.M. Vargas, F. Vielfaure, U.F. Schuchardt, J. Am. Oil Chem. Soc. 72 (1995) 1239–1241.
[67] G.J. Knothe, A. Kenar, Eur. J. Lipid Sci. Technol. 77 (2000) 489–493.
[68] M. Tariq, S. Ali, F. Ahmad, M. Ahmad, M. Zafar, N. Khalid, M.A. Khan, Fuel Process. Technol. 92 (2011) 336–341.
[69] G.W. Parshall, S.D. Ittel, Homogeneous Catalysis, Wiley, New York, 1992, pp. 269–296.
[70] A. Corma, L.T. Nemeth, M. Renz, S. Valencia, Nature 412 (2001) 423–425.
[71] M. Renz, T. Blasco, A. Corma, V. Fornés, R. Jensen, L. Nemeth, Chem. Eur. J. 8 (2002) 4708–4716.
[72] J. Holecek, K. Handlir, M. Nadvornik, A. Lycka, J. Organomet. Chem. 258 (1983) 147–153.
[73] J.T.B.H. Jastrzebski, G. Van Koten, Adv. Organomet. Chem. 35 (1993) 241–294.